This article is published in *The Plant Cell* Online, *The Plant Cell* Preview Section, which publishes manuscripts accepted for publication after they have been edited and the authors have corrected proofs, but before the final, complete issue is published online. Early posting of articles reduces normal time to publication by several weeks.

Methylation of Gibberellins by *Arabidopsis* GAMT1 and GAMT2 [W]

Marina Varbanova,[a] Shinjiro Yamaguchi,[b] Yue Yang,[a] Katherine McKelvey,[a] Atsushi Hanada,[b] Roy Borochov,[c] Fei Yu,[d] Yusuke Jikumaru,[b] Jeannine Ross,[e] Diego Cortes,[f] Choong Je Ma,[a] Joseph P. Noel,[e] Lew Mander,[g] Vladimir Shulaev,[f] Yuji Kamiya,[b] Steve Rodermel,[d] David Weiss,[c] and Eran Pichersky[a,1]

[a] Department of Molecular, Cellular, and Developmental Biology, University of Michigan, Ann Arbor, Michigan 48109-1048
[b] RIKEN Plant Science Center, Tsurumi-ku, Yokohama, Kanagawa 230-0045, Japan
[c] Smith Institute for Plant Sciences and Genetics, Faculty of Agriculture, Hebrew University, Rehovot 76100, Israel
[d] Department of Genetics, Development, and Cell Biology, Iowa State University, Ames, Iowa 50011-3260
[e] Howard Hughes Medical Institute, Jack H. Skirball Chemical Biology and Proteomics Laboratory, Salk Institute for Biological Studies, La Jolla, California 92037
[f] Virginia Bioinformatics Institute, Virginia Tech, Blacksburg, Virginia 24061
[g] Research School of Chemistry, Australian National University, Canberra ACT 0200, Australia

***Arabidopsis thaliana GAMT1* and *GAMT2* encode enzymes that catalyze formation of the methyl esters of gibberellins (GAs). Ectopic expression of *GAMT1* or *GAMT2* in *Arabidopsis*, tobacco (*Nicotiana tabacum*), and petunia (*Petunia hybrida*) resulted in plants with GA deficiency and typical GA deficiency phenotypes, such as dwarfism and reduced fertility. *GAMT1* and *GAMT2* are both expressed mainly in whole siliques (including seeds), with peak transcript levels from the middle until the end of silique development. Within whole siliques, *GAMT2* was previously shown to be expressed mostly in developing seeds, and we show here that *GAMT1* expression is also localized mostly to seed, suggesting a role in seed development. Siliques of null single *GAMT1* and *GAMT2* mutants accumulated high levels of various GAs, with particularly high levels of GA_1 in the double mutant. Methylated GAs were not detected in wild-type siliques, suggesting that methylation of GAs by GAMT1 and GAMT2 serves to deactivate GAs and initiate their degradation as the seeds mature. Seeds of homozygous *GAMT1* and *GAMT2* null mutants showed reduced inhibition of germination, compared with the wild type, when placed on plates containing the GA biosynthesis inhibitor ancymidol, with the double mutant showing the least inhibition. These results suggest that the mature mutant seeds contained higher levels of active GAs than wild-type seeds.**

INTRODUCTION

Gibberellins (GAs) form a large group of tetracyclic diterpenoid carboxylic acids, certain members of which function as natural regulators of a variety of growth and development processes in plants, such as germination, leaf expansion, stem elongation, bolting, flower induction, flower development, seed set, and fruit development (Davies, 1995). To date, >135 structurally distinct GAs have been identified from natural sources (http://www.plant-hormones.info/gibberellins.htm), most of which are not active in plants and may represent intermediates in the biosynthesis or degradation of bioactive GAs (Hedden and Phillips, 2000; Yamaguchi and Kamiya, 2000). In general, concentrations of active GAs in plants are highest in areas of rapidly elongating cells, such as stems, shoots, and developing seeds.

GA-deficient plants are extremely dwarfed in size and are often sterile or exhibit high rates of seed abortion, while plants that synthesize excess amounts of GAs are taller, with long, light-green leaves and decreased seed dormancy compared with wild-type seeds (Jacobsen and Olszewski, 1993; Huang et al., 1998). In *Arabidopsis thaliana*, the main bioactive GAs, GA_4 and GA_1 (Figure 1), have been shown to be involved in important aspects of plant development. Mutants with mildly reduced levels of GA_4 and GA_1 showed a semidwarf growth habit (Talon et al., 1990; Schomburg et al., 2003). GA_4 and GA_1 in *Arabidopsis* have been previously detected in seedlings, shoots, developing seeds, germinating seeds, and mature seeds.

The roles of GAs in developing and mature seeds are particularly intriguing. For example, it has been reported that during early seed development in many plant species, GA biosynthesis increases until the seeds mature, at which point the levels of active GAs begin to decrease in concert with the onset of dormancy (Kim et al., 2005; Swain et al., 1995). De novo biosynthesis of GAs is required during imbibition in some plant species, as was concluded from the observation that the presence of inhibitors of GA biosynthesis, such as paclobutrazol and tetcyclacis, prevented germination (Karssen et al., 1989; Schomburg et al., 2003). It is not clear whether active GAs synthesized during embryogenesis are degraded when the seed mature or whether they are stored for later use, and if so, what the storage form is and how they are converted back to active GAs.

[1] To whom correspondence should be addressed. E-mail lelx@umich.edu; fax 734-647-0884.
The author responsible for distribution of materials integral to the findings presented in this article in accordance with the policy described in the Instructions for Authors (www.plantcell.org) is: Eran Pichersky (lelx@umich.edu)
[W] Online version contains Web-only data.
www.plantcell.org/cgi/doi/10.1105/tpc.106.044602

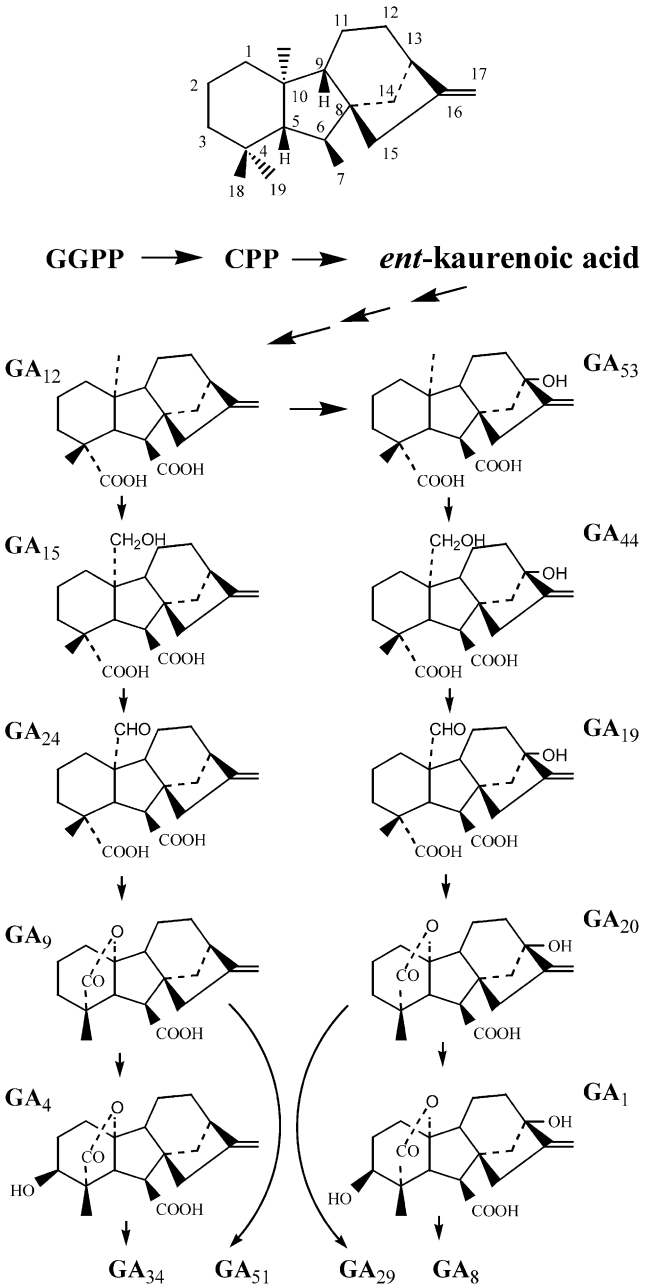

Figure 1. The GA Biosynthetic Pathway.

The pathway for biosynthesis of some active GAs, and their catabolic fates, are shown. GA_{34}, GA_{51}, GA_{29}, and GA_8 are catabolic products of GA degradation. The basic structure of *ent*-gibberellane with the numbering system of the carbons is shown at the top. GGPP, geranylgeranyl diphosphate; CPP, *ent*-copalyl diphosphate.

Deactivation mechanisms are necessary for effective regulation of bioactive hormone levels. So far, GA 2β-hydroxylation catalyzed by GA 2-oxidase has been the best-characterized GA deactivation reaction, which includes the conversions of GA_4 and GA_1 to GA_{34} and GA_8, respectively (Figure 1). GA 2-oxidases belong to the 2-oxoglutarate–dependent dioxygenase family (Thomas et al., 1999; Schomburg et al., 2003). Recently, another deactivation mechanism, involving epoxidation of the 16,17-double bond of GAs by a cytochrome P450 monooxygenase, has been found in rice (*Oryza sativa*) internodes (Zhu et al., 2006). Deactivation may also result from GA conjugation, which involves the formation of glucosyl ethers and esters (Schneider et al., 1992), although genes encoding these enzymes have not been identified yet.

Here, we report that two members of the SABATH methyltransferase gene family in the *Arabidopsis* genome, *GAMT1* and *GAMT2*, encode enzymes that use *S*-adenosine-L-methionine (SAM) as a methyl donor to methylate the carboxyl group of GAs, resulting in the methyl esters of GAs (MeGAs). Both genes are expressed most highly in the siliques during seed development. Siliques of GAMT1 and GAMT2 mutants show an increase in concentrations of GAs, and mature seeds of mutants appear to have higher concentrations of active GAs. Thus, methylation of GAs may constitute an additional mechanism for modulating cellular GA concentrations in addition to the oxidative pathways previously described (Thomas et al., 1999; Schomburg et al., 2003; Zhu et al., 2006).

RESULTS

Two Members of the *Arabidopsis* SABATH Family Methylate GAs

As part of a project aimed at identifying the substrates of each of the 24 carboxyl methyltransferases encoded by the SABATH gene family in *Arabidopsis* (Chen et al., 2003; D'Auria et al., 2003), we expressed full-length cDNAs of genes At4g26420 and At5g56300 in *Escherichia coli*, purified the proteins, and tested their activity with radioactive ^{14}C-SAM and a battery of potential substrates, using the methodology and array of substrates previously developed (Yang et al., 2006). Since the proteins belonging to these methyltransferases can methylate a deprotonated oxygen that is part of a carboxyl group, but cannot methylate the protonated oxygen on a hydroxyl group (Zubieta et al., 2003), the tested substrates included plant compounds with one or more carboxyl groups (Yang et al., 2006). In these high-throughput assays, GAMT1 (encoded by At4g26420) and GAMT2 (encoded by At5g56300) showed activity with GA_3, the one GA included in the high-throughput assay. No activity was observed with any other substrates included in this test.

Based on these initial results, we tested additional GAs, including four that are hydroxylated at position 13 (GA_1, GA_3, GA_{19}, and GA_{20}) and five that are not hydroxylated at this position (GA_4, GA_9, GA_{12}, GA_{34}, and GA_{51}) (Figure 1). These GAs have been previously detected in *Arabidopsis* (Talon et al., 1990; Huang et al., 1998; Eriksson et al., 2006). GAMT1 showed highest activity with GA_9 and GA_{20}, followed by GA_3, GA_4, GA_{34}, GA_{51}, and GA_1 (Table 1). GAMT2 methylated GA_4 with the highest efficiency, followed by GA_{34}, GA_9, GA_3, GA_1, GA_{51}, and GA_{20}. GAMT1 was able to methylate GA_{19} and GA_{12}, which do not contain a γ-lactone, albeit at a low rate, while GAMT2 did not act on these two GAs. Neither GAMT1 nor GAMT2 methylated additionally tested compounds with structural relatedness to GAs,

Table 1. Relative Activity of GAMT1 and GAMT2 with Several GAs

	Relative Activity (%)	
Substrate	GAMT1	GAMT2
GA_1	25	30
GA_3	80	45
GA_4	69	100
GA_9	100	60
GA_{12}	9	0
GA_{19}	19	0
GA_{20}	95	15
GA_{34}	46	80
GA_{51}	32	16

such as the diterpenes abietic acid and *ent*-kaurenoic acid. Products from the enzyme assays were verified to be methylated by comparing the retention time of the MeGA products with authentic standards on thin layer chromatography (TLC) and by gas chromatography–mass spectrometry after derivatization (see Supplemental Figure 1 online).

Enzymatic Properties of GAMT1 and GAMT2

The steady state kinetic parameters of each of the proteins were determined (Table 2). The K_m values of both enzymes with several GAs were in the range of 1.9 to 15.8 μM. GAMT1 had the lowest K_m value, 5.4 μM, with GA_4, and GAMT2 had the lowest K_m value, 1.9 μM, with GA_9. The K_m values for these enzymes with SAM in combination with various GAs were in the range of 30 to 50 μM. All these K_m values and the observed K_{cat} values (Table 2) are similar to those obtained for other SABATH methyltransferases with their in vivo substrates (Ross et al., 1999; Zubieta et al., 2003). The pH optimum of GAMT2 was determined to be 8.0, whereas the pH optimum for GAMT1 was 7.5. The cations K^+ and NH_4^+ in concentration of 5 mM were found to increase the activity of GAMT1 by threefold and fourfold, respectively, while Zn^{2+}, Cu^{2+}, Fe^{2+}, and Fe^{3+} at this concentration inhibited >90% GAMT1 activity. GAMT2 activity was not enhanced nor inhibited by K^+, NH_4^+, Na^+, Ca^{2+}, Fe^{2+}, Mg^{2+}, and Mn^{2+} but was inhibited similarly to GAMT1 by Fe^{3+}, Zn^{2+}, and Cu^{2+}.

Protein Sequences of GAMT1 and GAMT2

GAMT1 and *GAMT2* are part of the SABATH methyltransferase family with 24 members in *Arabidopsis* (Chen et al., 2003; D'Auria et al., 2003). *GAMT1* encodes a protein of 376 amino acids, with a calculated molecular mass of 41.5 kD, and *GAMT2* encodes a protein of 388 amino acids, with a calculated molecular mass of 43.3 kD. The *Arabidopsis* enzyme with the most similar sequence to GAMT1 within this family is GAMT2, and vice versa. An alignment of the sequences indicates that they are 58% identical (Figure 2). The next most similar *Arabidopsis* protein, with 34% identity to both GAMT1 and GAMT2, is IAMT1, an enzyme that is capable of methylating auxin (indole-3-acetic acid [IAA]) to produce methyl IAA (Zubieta et al., 2003; Qin et al., 2005). It should be noted that the current annotation of *GAMT1* (At4g26420) on The Arabidopsis Information Resouce (TAIR) website (http://www.arabidopsis.org/) shows a third intron occurring toward the end of the third exon shown in Figure 3A, then a fourth exon, a fourth intron, and a fifth exon. Such a gene would encode a protein of 620 amino acids, with a calculated molecular mass of 68.2 kD. There are multiple lines of evidence indicating that this annotation is erroneous. First, all the full-length clones that we have isolated, as well as the full-length clones shown on the TAIR website, support the three-exon, two-intron structure shown in Figure 3A, encoding the protein whose sequence is shown in Figure 2 (this is the protein whose biochemical characterization is presented here). Furthermore, all SABATH methyltransferases, including the GAMT1 protein encoded by the three-exon, two-intron gene shown in Figure 3A, are ~350 to 400 amino acids long. Finally, the GAMT1 protein in the plant, as detected by antibodies specific to GAMT1, migrates on SDS-PAGE gel as an ~40-kD protein (Figure 3C), a mass consistent with the calculated molecular mass (41.5 kD) of the GAMT1 protein encoded by the gene whose structure is shown in Figure 3A but inconsistent with the present annotation in TAIR. The updated annotation of At4g26420 will be available from TAIR and the National Center for Biotechnology Information (NCBI) following the next genome release (TAIR7) scheduled for January, 2007.

Overexpression of *Arabidopsis GAMT1* and *GAMT2* in *Arabidopsis*, Tobacco, and Petunia Plants Results in Dwarf Phenotypes

We obtained *Arabidopsis* plants that expressed *GAMT1* and *GAMT2* under the control of the 35S cauliflower mosaic virus promoter. We also obtained an *Arabidopsis* line in which an enhancer tag was inserted upstream of the *GAMT1* gene (Weigel et al., 2000; Yu et al., 2004). The majority of independently obtained transgenic *Arabidopsis* lines (>10) expressing *GAMT1* either under the control of the 35S promoter or the enhancer tag (verified by RT-PCR and RNA gel blot analysis; data not shown) exhibited a similar phenotype that included small, dark-green rosette leaves (Figure 4A) that grew exceedingly slow, and they developed into dwarfed, bushy plants (Figure 4B). Some never bloomed, and those that did bloom started doing so after 3 months (whereas wild-type plants under these conditions began blooming in 6 weeks). Their flowers were small and mostly sterile. Spraying plants with GA_4 recovered some fertility and caused partial amelioration of the dwarf phenotype of the whole plant. Spraying with $MeGA_4$ did not ameliorate the dwarf phenotype.

A similar phenotype was observed in transgenic tobacco (*Nicotiana tabacum*) and petunia (*Petunia hybrida*) plants expressing *GAMT1* under the control of the 35S promoter (Figure 5). The

Table 2. Kinetic Parameters of GAMT1 and GAMT2

	K_m (μM)	K_{cat} (s^{-1})	K_{cat}/K_m ($nM^{-1}\ s^{-1}$)
GAMT1			
GA_4	5.4	1.0×10^{-2}	1.8
GA_9	15.8	2.6×10^{-2}	1.6
GAMT2			
GA_4	5.9	1.5×10^{-3}	0.2
GA_9	1.9	1.8×10^{-3}	0.9

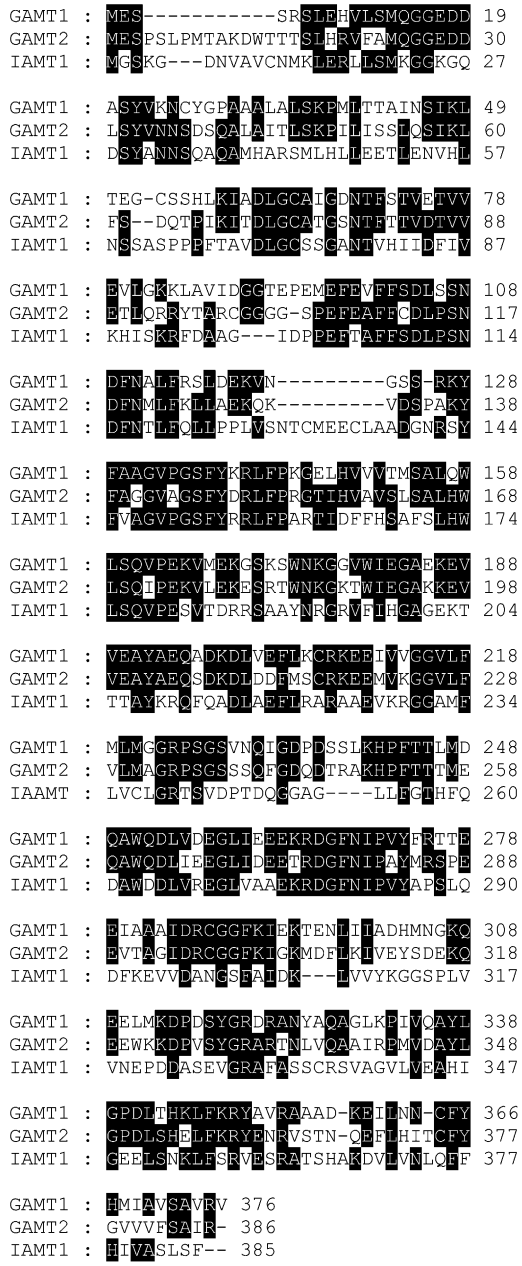

Figure 2. Alignment of the Protein Sequences of *Arabidopsis* GAMT1, GAMT2, and IAMT1.

Residues at a given position that are identical in at least two of the three proteins are shown in white letters on black background. IAMT1 is encoded by gene At5g55250. The sequences of the proteins and the genes encoding them can be accessed at http://www.biology.lsa.umich.edu/research/labs/pichersky/2010%20NSF/database/database1.htm.

transgenic tobacco plants were slow growers and had small flowers with reduced seed set. The petunia plants bloomed only under long-day conditions, and the flowers were small and sterile.

Expression of *GAMT2* in transgenic *Arabidopsis* plants under the control of the 35S promoter did not produce a dwarf phenotype at the early stage of plant development when grown on Murashige and Skoog (MS) medium, and seedlings were indistinguishable from wild-type seedlings. However, after transfer to soil on the third week after germination, the majority of transgenic plants (>10 independent lines) showed a different growth pattern from the wild type, growing slowly and exhibiting a higher number of branches compared with wild-type plants, giving them a semidwarf, bushy look (Figure 4C). While some of these plants had reduced fertility, the majority had normal seed set. The differences in the phenotypes of *GAMT2*-overexpressing lines and *GAMT1*-overexpresing lines persisted under different light regimes.

GAMT1- and *GAMT2*-Overexpressing Lines Are Deficient in GAs

To verify whether overexpression of *GAMT* genes caused GA deficiency in *Arabidopsis* plants, we measured endogenous levels of precursor and bioactive GAs in aerial parts of *GAMT1*- and *GAMT2*-overexpressing plants just after the start of flowering. As shown in Table 3, the levels of GA_4, the major bioactive form at this stage in *Arabidopsis*, were much lower in plants overexpressing *GAMT1* (<10%) than those in wild-type plants. In addition, all precursor GAs that we measured were less abundant in *GAMT1* overexpression lines than in wild-type controls. Plants overexpressing *GAMT2* contained lower levels of bioactive GA_4 than did wild-type plants, but in general, the depletions of endogenous GAs in *GAMT2*-overexpressing lines was not as severe as those in *GAMT1*-overexpressing lines, and some GAs showed no difference in levels with control or even higher levels (e.g., GA_{15}). These results are consistent with the interpretation that the dwarfed and semidwarfed phenotypes of plants overexpressing *GAMT1* and *GAMT2*, respectively, are attributable to reductions in bioactive GA levels.

GAMT1 and *GAMT2* Are Expressed in Developing Seeds in *Arabidopsis*

The results described above indicated that *Arabidopsis* possesses enzymes capable of methylating GAs. To determine the role of these enzymes in the plant, we next examined the expression profile of the two genes encoding these enzymes. Quantitative RT-PCR (qRT-PCR) was performed on RNA isolated from cauline and rosette leaves, stem, flowers, roots, siliques (including seeds), germinating seeds, and 2-week-old seedlings. Little expression of either of these two genes was observed in tissues other than siliques (Figure 6), with the exception of weak but detectable expression in germinating seeds. Examination of the levels of *GAMT1* and *GAMT2* transcripts from siliques at different stages of development (Bowman, 1994) showed that expression of both genes began at early stages of silique development, peaked in the second half of this process, and then began to decrease after the start of desiccation (Figure 6). Germinating seeds contained detectable levels of *GAMT1* and *GAMT2* transcripts, but they were much lower than the maximum levels in developing siliques.

We also performed immunoblot measurements of the levels of GAMT1 protein in different *Arabidopsis* organs using polyclonal

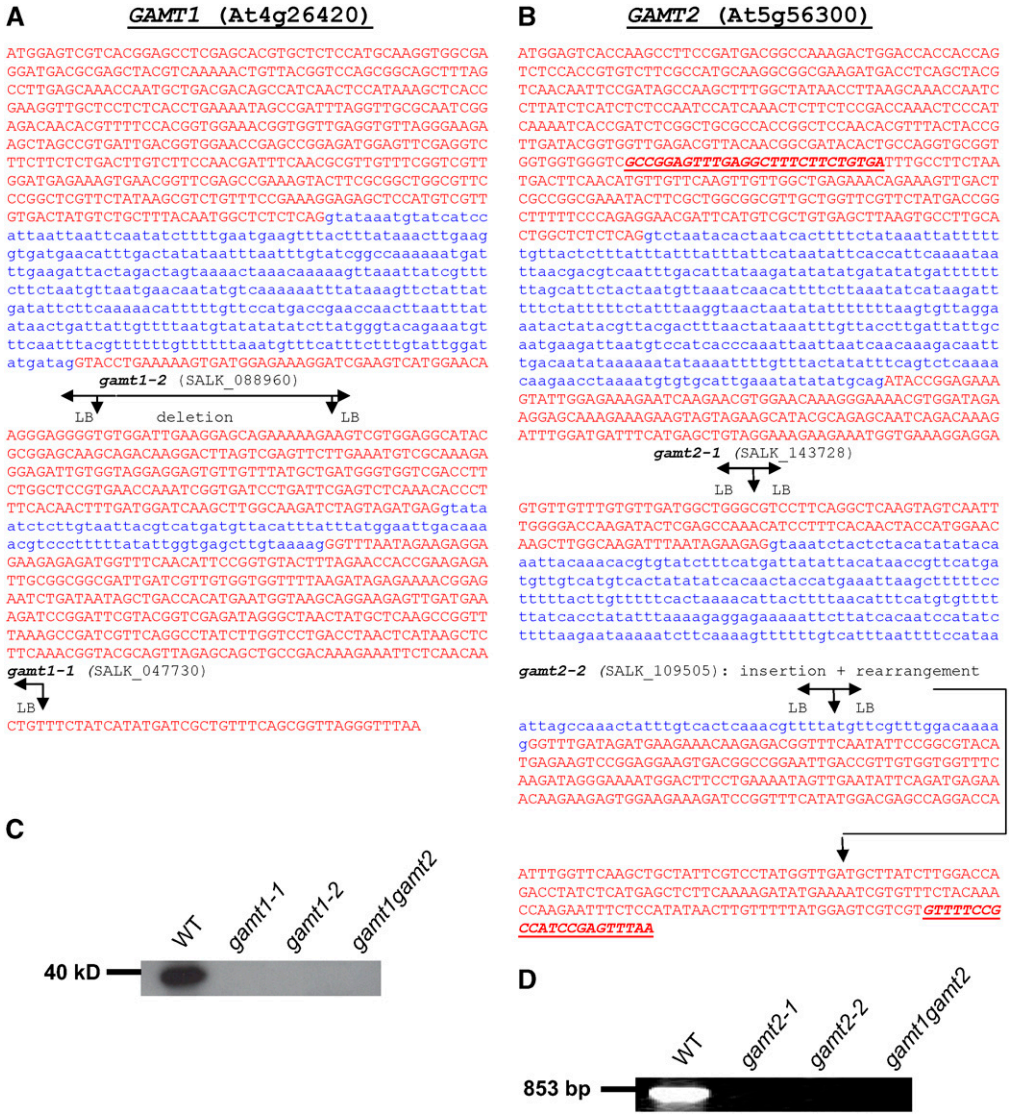

Figure 3. Analysis of T-DNA Insertional Mutants in *GAMT1* and *GAMT2*.

(A) The correct gene structure of GAMT1 (At4g26420) based on comparisons of full-length cDNAs with the genomic sequence. Exon sequences are shown in red, and intron sequences are shown in blue. The position of the T-DNA insertions in *gamt1-1* and *gamt1-2* are shown based on sequencing of the amplified border segments. In *gamt1-2*, a left border (LB) is present at both ends of the T-DNA insertion, and the genomic sequence in between has been deleted.

(B) The gene structure of *GAMT2* (At5g56300) based on the annotation in TAIR and the comparisons of full-length cDNAs with the genomic sequence. The position of the T-DNA insertions in *gamt2-1* and *gamt2-2* are shown based on sequencing of the amplified border segments. In *gamt2-2*, the region downstream from the insertion is rearranged so that the outlined part of the third exon is missing and a segment of intron 2 plus additional unknown segments are present. The bold and underlined sequences indicate the position of the primers used in the RT-PCR experiment whose results are shown in **(D)**.

(C) A protein gel blot using anti-GAMT1 antibodies with crude protein extracts from siliques of wild-type plants, *gamt1-1*, *gamt1-2*, and the double mutant *gamt1-2 gamt2-2*. The GAMT1 protein, present in the wild-type plants but not in the mutants, migrates on SDS-PAGE gels as an ~40-kD protein.

(D) Results of RT-PCR using the oligonucleotide primers indicated in **(B)** and RNA extracted from siliques of wild-type plants and *gamt2-1*, *gamt2-2*, and *gamt1-2 gamt2-1*. The predicted product of 853 nucleotides was obtained from wild-type plants but not from mutants.

antibodies specific against GAMT1 (these antibodies did not react with GAMT2 protein extracted from the plant [Figure 3C] or with GAMT2 protein produced in *E. coli* [data not shown]; raising antibodies against GAMT2 was not successful). The results of these immunoblots (Figure 7A) were consistent with the qRT-PCR results, showing the presence of the protein in siliques only. A more detailed examination of the levels of GAMT1 protein in developing siliques at different stages of development showed that protein levels closely correlated with GAMT1 transcript levels, peaking toward the end of the developmental process of the silique (Figure 7B).

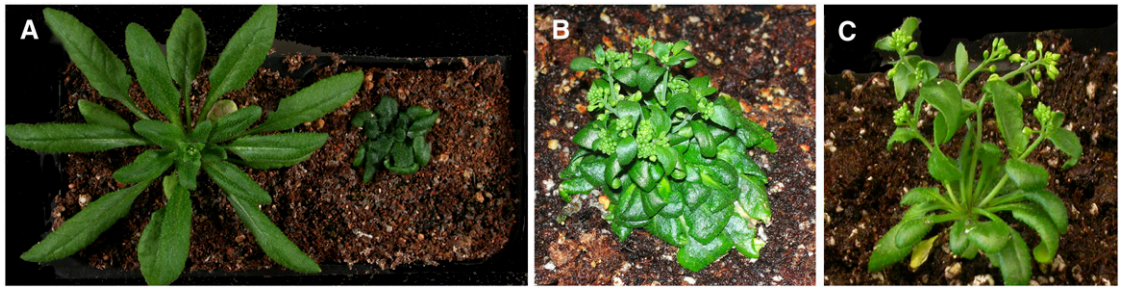

Figure 4. Phenotypes of *Arabidopsis* Col-0 Overexpressing *GAMT1* and *GAMT2*.

(A) A 4-week-old *Arabidopsis* wild-type plant (left) next to a same-age plant overexpressing *GAMT1* due to enhancer tagging.
(B) A 3-month-old plant overexpressing *GAMT1* due to enhancer tagging, showing the bushy, dwarf phenotype.
(C) A 2-month-old flowering *Arabidopsis* plant overexpressing *GAMT2* under the control of the 35S promoter, showing the bushy, semidwarf phenotype with very small flowers.
All plants are shown to roughly equal scale.

Plants expressing a β-glucuronidase (GUS) reporter gene under the control of the *GAMT1* promoter (*GAMT1-GUS*) and stained for GUS activity showed staining in the developing seeds and in the anthers (Figures 8A to 8D). In later stages of seed development, some GUS staining was also observed in the septum and in the funiculus as well (Figure 8E). GUS staining of transgenic plants with a *GAMT2* promoter–*GUS* fusion gene indicated expression in the anthers but, in contrast with the qRT-PCR results, no staining in the developing seeds (data not shown).

Siliques of Mutant Plants Have Higher Levels of GAs Than Wild-Type Plants

We obtained *Arabidopsis* Columbia (Col) plants that contained T-DNA insertions in *GAMT1* and *GAMT2* (Figure 3). *gamt1-1* had an insertion in exon 3, and *gamt1-2* had an insertion in exon 2 that included a small deletion of the coding region (Figure 3A). Lines homozygous for either *gamt1-1* or *gamt1-2* produced no GAMT1 protein (Figure 3C). *gamt2-1* had an insertion in exon 2 (Figure 3B), and *gamt2-2* had an insertion intron 2 that caused a partial deletion and rearrangement of exon 3 (Figure 3B). Lines homozygous for either mutation contained no functional transcript (Figure 3D). In addition, we obtained the homozygous double mutant line by crossing *gamt1-2* and *gamt2-2* mutants. None of the single mutant or double mutant plants showed visible phenotypes, such as altered germination rate, growth habit, or seed set, under normal growth conditions. These verified null mutants (Figures 3C and 3D) grew normally and had no visible morphological differences with wild-type plants.

We measured the content of some GAs in the siliques of homozygous *gamt1-2*, *gamt2-2*, and *gamt1-2* × *gamt2-2* plants using siliques of developmental stages 5, 6, and 7, where *GAMT1* and *GAMT2* expression levels are close to or at their highest. The levels of bioactive GA_4 and GA_1 in siliques were significantly higher in the *gamt1 gamt2* double mutant than those in wild-type plants, with the level of GA_1 especially elevated in the double mutant (~10-fold) compared with that in the wild type (Figure 9). GA_4 and GA_1 levels were slightly more abundant in *gamt1* and

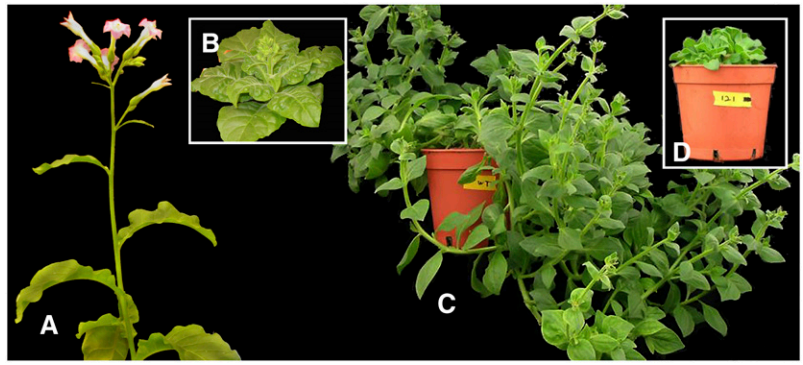

Figure 5. Phenotypes of Petunia and Tobacco Plants Overexpressing *GAMT1* under the Control of the 35S Promoter.

(A) Tobacco wild-type plant.
(B) A tobacco plant of the same age as in **(A)** expressing *GAMT1* under the control of the 35S promoter.
(C) Petunia wild-type.
(D) A petunia plant of the same age as in **(C)** expressing *GAMT1* under the control of the 35S promoter.

Table 3. Endogenous GA Levels in *Arabidopsis* Plants Overexpressing *GAMT1* or *GAMT2*

		Wild-Type Control for *GAMT1*-OE[a]	*GAMT1*-OE Line 13-5[a]	*GAMT1*-OE Line 13-6[a]	Wild-Type Control for *GAMT2*-OE[b]	*GAMT2*-OE Line 12-3[b]	*GAMT2*-OE Line 12-5[b]
13-H GAs	GA_{12}	15.4/13.2	0.7/4.1	4.3/1.2	21.5/14.0	16.9/10.2	10.7/15.0
	GA_{15}	1.5/3.2	0.2/1.3	0.4/1.2	4.4/1.7	10.8/7.8	11.8/10.6
	GA_{24}	–/21.7	–/2.9	–/2.9	24.6/16.9	14.6/10.8	10.7/15.2
	GA_9	0.4/ND	0.1/ND	0.1/ND	ND/ND	ND/ND	ND/ND
	GA_4	0.8/2.3	0.1/0.1	ND/0.1	0.9/0.4	0.1/0.1	0.2/0.2
13-OH GAs	GA_{53}	2.4/2.4	0.6/0.4	0.1/0.3	2.8/1.6	1.4/1.1	0.6/1.0
	GA_{44}	ND/ND	ND/ND	ND/ND	ND/ND	ND/ND	ND/ND
	GA_{19}	–/16	–/3.6	–/2.9	8.2/3.0	9.5/6.3	8.2/10.5
	GA_{20}	0.4/0.4	0.1/ND	0.1/ND	0.1/ND	0.1/ND	0.1/0.1
	GA_1	0.2/0.5	ND/ND	ND/ND	ND/ND	ND/ND	ND/ND

GA measurements were performed twice using independently prepared plant materials. Values (ng/g dry weight) from both the first (left) and second (right) measurements are shown. –, Detectable, but could not be quantified reliably due to comigration of impurities. ND, not detected or could not be quantified reliably due to low abundance.

[a,b] These two sets of plant materials were grown on different occasions. OE, overexpressing.

gamt2 single mutants than in wild-type plants as well (Figure 9). The effects of *gamt* single and/or double mutations were observed on the levels of the deactivated forms GA_{34} and GA_8 and on some precursor GAs in the *gamt1* plants. These results support the conclusion that GAs are endogenous substrates for GAMT1 and GAMT2 in wild-type siliques.

Analysis of Endogenous MeGAs

To our knowledge, MeGAs have not been identified as endogenous compounds in angiosperms. Elevated GA levels in siliques of *gamt* mutants suggested that MeGAs were produced by GAMTs and that they might accumulate in wild-type siliques. To address this question, we analyzed endogenous $MeGA_1$, $MeGA_4$, and $MeGA_{20}$ using isotope-labeled MeGAs as internal standards by gas chromatography–selected ion monitoring (GC-SIM). We chose these MeGAs to be analyzed because the levels of the corresponding free GAs increased in the *gamt1 gamt2* mutant (Figure 9) and/or because they were preferred substrates of at least one of the GAMTs in vitro (Table 1). Using the procedure detailed in the Supplemental Methods online, we were able to purify and detect all isotope-labeled MeGAs added to the extracts. However, none of the endogenous ones was detected in wild-type and *gamt1 gamt2* mutant (included as a control) siliques (see Supplemental Figure 2 online). We also analyzed these MeGAs in plants overexpressing *GAMT1* (lines 13-5 and 13-6; Table 3) and wild-type plants (as a control) just after flowering. Again, endogenous MeGAs were undetectable, while all internal standards were detected.

GAMT1 and *GAMT2* Mutants Display an Excess GA Phenotype in the Seeds

The expression profiles of *GAMT1* and *GAMT2* suggest that the enzymes they encode play a specific role during seed development. To examine the effect of the methylation of GAs in *Arabidopsis* seeds, the homozygous single and double mutant seeds were placed on plates containing MS basal medium that was supplemented with ancymidol, an inhibitor of GA biosynthesis (Rademacher, 2000). Differences in germination rates were observed between mutants and wild-type plants. Germination (defined as the appearance of the radicle) of wild-type seeds was not inhibited by 10 μM concentration of ancymidol but was ~90% inhibited by the presence of 20 μM concentration of ancymidol and completely inhibited at 30 μM (Figure 10). By contrast, at 30 μM ancymidol, 25 to 60% of the single and the double mutant seeds still germinated, with the double mutant seeds showing the highest germination rate (Figure 10), and their cotyledons were green, although they eventually stopped growing. Some germination of the single and double mutants was still observed at 40 μM concentration of ancymidol in the medium. Consistent with these results, germination of seeds from plants

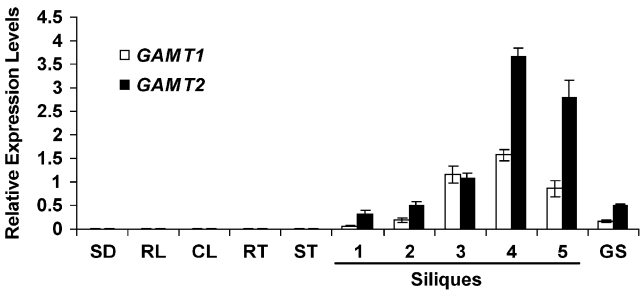

Figure 6. Detection of *GAMT1* and *GAMT2* Transcripts in Different *Arabidopsis* Organs and Stages of Seed Development by qRT-PCR.

Relative levels of *GAMT1* and *GAMT2* transcripts (compared with levels of transcripts of the control, the *ubi10* gene) are presented as mean values ± SD, calculated from three sets of independent experiments. Silique samples are as follows: 1, flower buds and stage 1 siliques; 2, stages 2 and 3; 3, stages 4 and 5; 4, stages 6, 7, and 8; 5, stages 9 and 10. The 10 stages of the siliques were defined according to Bowman (1994), and they span the development process from the smallest silique (stage 1) to fully mature and dry siliques (stage 10). SD, 2-week-old seedlings; RL, rosette leaf; CL, cauline leaf; RT, root; ST, stem; GS, germinating seeds.

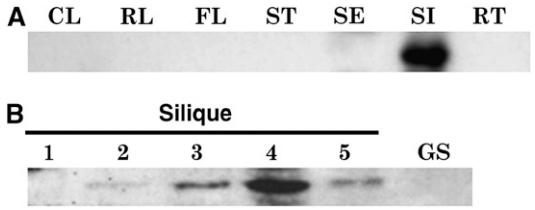

Figure 7. Levels of GAMT1 Protein in Different Tissues and Developmental Stages of *Arabidopsis* Plants.

(A) Immunoblot analysis of the distribution of GAMT1 protein in different plant organs using anti-GAMT1 antibodies. CL, cauline leaf; RL, rosette leaf; FL, flower; ST, stem; SD, 2-week-old seedlings; SI, siliques (stages 6, 7, and 8); RT, root.
(B) Immunoblot analysis of GAMT1 in different stages of silique development and in germinating seeds. Lanes 1 to 5 are samples from siliques of same stages denoted by samples 1 to 5 in Figure 6. GS, germinating seeds.

overexpressing *GAMT1*and *GAMT2* with the 35S promoter was 85% inhibited by 10 μM ancimydol, and germination of seeds from plants expressing *GAMT1* via an enhancer tag was inhibited 50% (Figure 10).

DISCUSSION

Arabidopsis At4g26420 and At5g56300 Encode GA Methyltransferases That Are Expressed Predominantly in Siliques

GAMT1 and GAMT2, which we have shown here to methylate the carboxyl group of various GAs to form the corresponding MeGA esters, belong to the plant SABATH family of methyltransferases. This family also includes enzymes that methylate the carboxyl group of other growth substances, such as salicylic acid (SA), jasmonic acid (JA), and auxin (IAA), to form the respective methyl esters MeSA, MeJA, and MeIAA (Ross et al., 1999; Seo et al., 2001; Zubieta et al., 2003). The *Arabidopsis* genome has 24 genes belonging to this family (Chen et al., 2003; D'Auria et al., 2003), and among the proteins encoded by these 24 genes, GAMT1 and GAMT2 are the most similar proteins to each other. The level of divergence between GAMT1 and GAMT2 proteins (58% identity) indicates that the duplication that gave rise to the genes encoding them (At4g26420 and At5g56300) is not very recent.

We show here that *GAMT1* and *GAMT2* both are expressed primarily in developing siliques, with peak transcript levels toward the end of this process. Our qRT-PCR results concerning the expression of *GAMT2* are consistent with data obtained from microarray experiments and available online (Zimmermann et al., 2004; https://www.genevestigator.ethz.ch; Schmid et al., 2005; http://www.weigelworld.org/resources/microarray/AtGenExpress/). Because of the mistake in the annotation of *GAMT1* in TAIR, and the fact that based on this erroneous annotation all 11 oligonucleotides chosen by Affimatrix to represent *GAMT1* on the ATH1 microarray are derived from sequences downstream of *GAMT1* that are not part of the *GAMT1* gene, there is no relevant information on the expression of *GAMT1* on these websites. Nonetheless, our qRT-PCR measurements of *GAMT1* transcripts showed that this gene has a very similar pattern of expression to *GAMT2* throughout the developmental process of the siliques, with little expression seen elsewhere. Measurements of GAMT1 protein levels by protein blotting experiments with GAMT1-specific antibodies were consistent with the qRT-PCR results.

Staining of siliques of transgenic plants expressing GUS under the control of the *GAMT1* promoter indicated expression mostly in the developing seeds. We did not observe any GUS staining in the developing seeds of the transgenic plants carrying the *GAMT2* promoter–GUS fusion gene, but this might have been the result of an incomplete promoter segment being used, as data provided on both https://www.genevestigator.ethz.ch and http://www.weigelworld.org/resources/microarray/AtGenExpress/

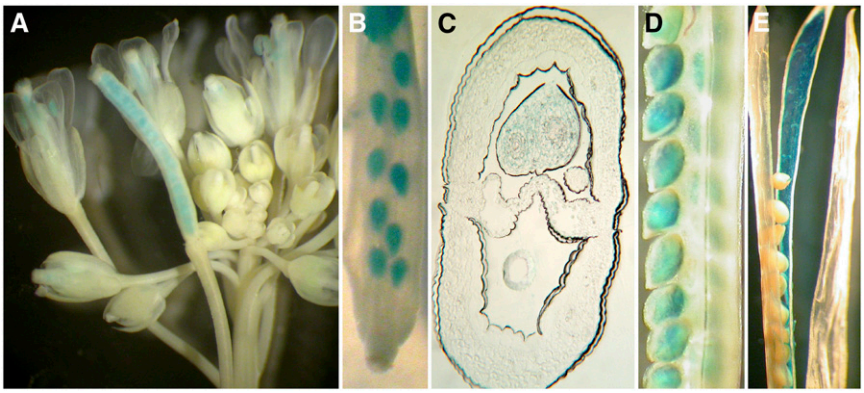

Figure 8. Staining for GUS Activity with Plants Transgenic for the *GAMT1* Promoter–*GUS* Transgene.

(A) Inflorescence with flowers and siliques at different stages of development.
(B) A young silique showing staining in the developing seeds.
(C) Cross section of a developing seed.
(D) Maturing seeds.
(E) A mature silique showing staining in the septum and funiculus.

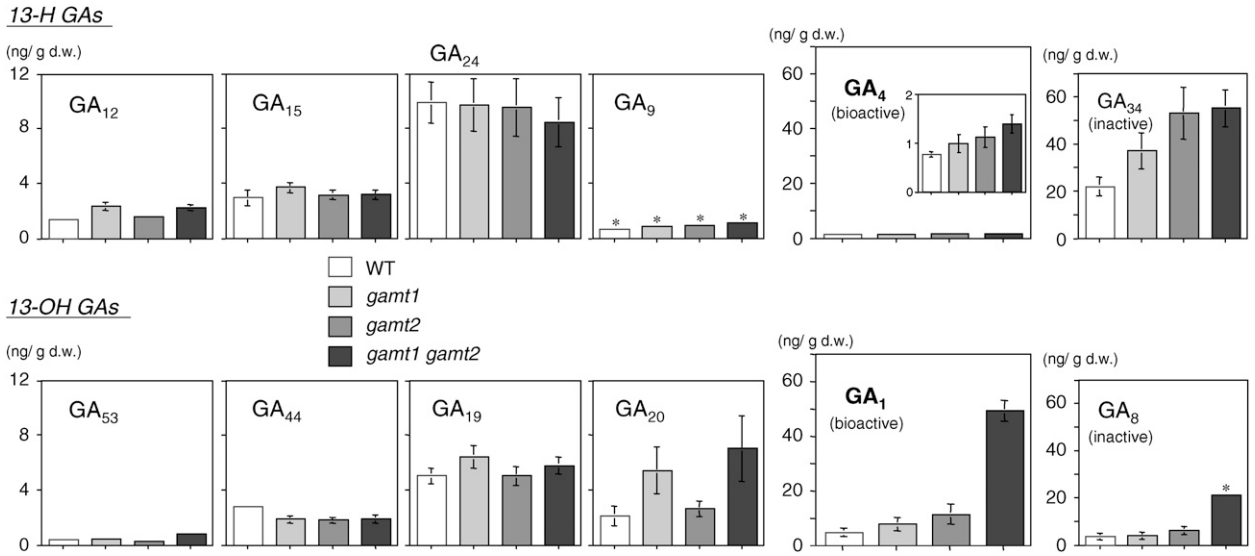

Figure 9. GA Levels in Developing Siliques of *gamt* Single and Double Mutants.

Shown are endogenous levels of GAs in developing siliques of the wild type, *gamt1-1* and *gamt2-2* single mutants, and the *gamt1-2 gamt2-2* double mutant plants. Results of respective GAs are displayed according to their order in the biosynthesis pathway (see Figure 1). Results of GA_4 are also indicated in the inset with a different *y* axis scale to clarify the differences among the genotypes. Note that the *y* axis scale for precursor GAs (GA_{12}, GA_{15}, GA_{24}, GA_9, GA_{53}, GA_{44}, GA_{19}, and GA_{20}) is different from that for bioactive (GA_4 and GA_1) and deactivated (GA_{34} and GA_8) forms. GA measurements were conducted three times using independently prepared plant extracts. Means with SE (which are displayed only when they are >0.2) from triplicates are shown. Asterisks indicate that these GAs could be measured reliably only once due to comigration of impurities on the liquid chromatograph. d.w., dry weight.

indicate expression specifically in seeds, in addition to expression in whole siliques.

In in vitro assays, GAMT1 and GAMT2 methylated the carboxyl group (position 7) of a variety of GAs to produce the corresponding methyl esters. While we did not test all possible GAs, the results obtained with the substrates we used indicated that both enzymes have a broad specificity, although GAMT1 appears to have somewhat broader specificity (Table 1). Transgenic *Arabidopsis* plants overexpressing either *GAMT1* or *GAMT2* show depletion in various GAs (Table 3), as would be expected if GAs were the substrates of these enzymes. While the specific level of depletion of each GA depends on a complex set of parameters, including the internal concentrations of each GA, the internal concentration of the methyltransferase, the K_m values of each enzyme for each substrate, and the flux of the biosynthetic and catabolic pathways that interconvert all these GAs, some correlations between depletion levels and preference of the enzymes for specific substrates could be discerned. For example, GAMT1 appears to have a higher activity with GA_{20} than GAMT2 does, and the depletion of GA_{20} in the *GAMT1*-overexpressing lines is more noticeable than in *GAMT2*-overexpressing lines. However, this correlation is not perfect and with our present limited

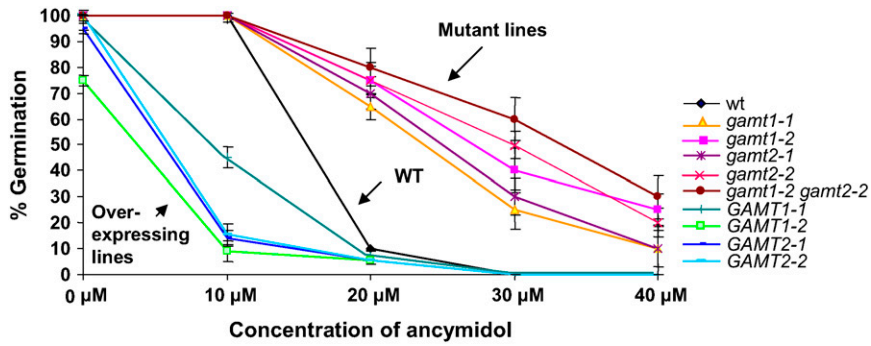

Figure 10. Inhibition of Seed Germination by Ancymidol.

Seeds were germinated on MS plates containing the indicated concentration of ancymidol. *GAMT1-1* is the enhancer-tagged line overexpressing *GAMT1*, *GAMT1-2* is the *GAMT1*-overexpressing line 13-5 (Table 1), and *GAMT2-1* and *GAMT2-2* are two independent *GAMT2*-overexpressing lines 12-3 and 12-5, respectively. Values are means ± SD calculated from three sets of independent experiments.

knowledge may be too difficult to predict. In addition, several genes encoding enzymes in the late stage of GA biosynthesis have been shown to be under negative feedback regulation via bioactive GAs. Therefore, the observed decrease in the levels of some precursor GAs in *GAMT*-overexpressing plants might be due to increased GA 20-oxidase activity as a consequence of reduced GA_4 levels. So, while the clear phenotypic differences between *Arabidopsis* plants overexpressing *GAMT1* and *GAMT2*, which are correlated with less severe reduction in active and nonactive GAs in *GAMT2* overexpressors compared with *GAMT1* overexpressors, are most likely due to the differences in enzymatic activities of the two enzymes with various GAs, the direct causes of these differences are difficult to identify at this point.

An even stronger indication that GAs are the endogenous substrates of GAMT1 and GAMT2 is the observation that in *gamt1*, *gamt2*, and *gamt1 gamt2* mutant lines, the levels of several GAs in the siliques, and in particular the levels of the active GA_1 and GA_4, are higher than in the siliques of wild-type plants. Here, too, a general but imperfect correlation is seen between increases in levels of individual GAs and the relative activity levels of GAMT1 and GAMT2 with these compounds. For example, GAMT1 has strong in vitro activity with GA_{20}, and *gamt1* shows increased levels of GA_{20} in silqiues, while GAMT2 has weak activity with GA_{20} in vitro, and the *gamt2* mutant shows little or no differences in GA_{20} levels in siliques. In some cases, when both enzymes appear to have similar activity with a given GA, for example GA_1, the level of this GA increases only a little in either *gamt1* or *gamt2*, while the level of this GA is much increased in the *gamt1 gamt2* double mutant.

Curaba et al. (2004) reported that the level of GA_1 was similar to that of GA_4 in the developing *Arabidopsis* seeds, unlike in other *Arabidopsis* tissues that were found to contain higher levels of GA_4 than those of GA_1, including vegetative organs, flowers, and germinating seeds (Talon et al., 1990; Huang et al., 1998; Ogawa et al., 2003; Schomburg et al., 2003; Fei et al., 2004). Our results here show that GA_1 was more abundant than GA_4 in developing siliques (including seeds) of wild-type plants (Figure 9). Interestingly, the level of GA_1 was drastically elevated, whereas that of GA_4 increased only slightly in siliques of *gamt1 gamt2* mutant plants compared with wild-type siliques (Figure 9). These differences in the levels of GA_4 and GA_1 among the genotypes cannot be readily explained by the substrate specificity of GAMTs because their recognition of the 13-hydroxyl group does not appear to be strict in vitro (Table 1). These results suggest an unknown mechanism that allows accumulation of GA_1 specifically in developing siliques and/or seeds; possibly, GA 13-oxidase (for which the gene has not yet been identified) and GA catabolic enzymes that strictly distinguish the 13-hydroxyl group (such as GA 16,17-epoxidase of rice; Zhu et al., 2006) might be involved in this mechanism.

We chose to measure GAs in siliques at the developmental stage in which GAMT1 and GAMT2 show peak expression to maximize differences between wild-type and mutant plants. We therefore do not know the exact concentrations of GAs in the mature seeds. However, the observation that the germination of *gamt1* and *gamt2* mutant seeds is inhibited less by the GA biosynthesis inhibitor ancymidol (a pyrimidine that acts as an inhibitor of monoxygenases catalyzing the oxidative step from *ent*-kaurene to *ent*-kaurenoic acid; Rademacher, 2000) (Figure 10) suggests that the mature seeds of the mutants also contain higher levels of active GAs than in the wild-type seeds and are thus capable of initiating germination without de novo GA biosynthesis. Alternatively, weak but detectable expression of *GAMT1* and *GAMT2* genes in germinating seeds revealed by qRT-PCR (Figure 6) suggests that these methyltransferases might be involved in GA deactivation in imbibed seeds as well. If this was the case, the observed differences in germination rates among the genotypes in the presence of ancymidol (Figure 10) might be due to the effect of *gamt* mutations on GA levels after the start of imbibition.

Putative Role of GA Methylation in Seed Development and Germination

It is generally known that GAs are synthesized during seed development and during germination (Ogawa et al., 2003), but little is known about the distribution and specific roles of GAs in *Arabidopsis* developing siliques and seeds (Curaba et al., 2004; Kim et al., 2005). In pea (*Pisum sativum*), an active GA, GA_1, is found in high levels in the seeds (4 to 7 d after anthesis) and at lower levels in the pod (MacKenzie-Hose et al., 1998). It has also been reported that exchange of hormones in the fruit between the pod and the seeds is necessary for proper seed development in *P. sativum* and that lack of sufficient levels of GAs in either the pod or in the embryo leads to seed abortion (Eeuwens and Schwabe, 1975; MacKenzie-Hose et al., 1998).

Although most enzymes of the GA biosynthetic pathway and the enzymes for the catabolic pathway have been identified (Hedden and Kamiya, 1997; Olszewski et al., 2002), roles of many of these enzymes in plant development remain to be fully characterized. In particular, while several homologous 2β-oxidases that can deactivate GAs have been identified in *Arabidopsis* (Thomas et al., 1999; Schomburg et al., 2003; Wang et al., 2004) and some of these show expression in developing seeds, a physiological role in GA deactivation in the seeds for these oxidases has not yet been fully established. In pea, the importance of GA deactivation has been shown by the phenotypic and biochemical studies of the *slender* (*sln*) mutant, which lacks a GA 2-oxidase that is involved in the conversion of GA_{20} to GA_{29} during seed development (Lester et al., 1999; Martin et al., 1999). In the *sln* mutant, GA_{20} accumulates to a high level in mature seeds and then is converted to GA_1 upon germination, resulting in a GA overproduction phenotype during seedling growth.

Methyl esters of GAs have been shown to be inactive in several angiospermous species (Weiss et al., 1995; Cowling et al., 1998), and $MeGA_4$ did not bind significantly to the soluble receptor GID1 from rice (Ueguchi-Tanaka et al., 2005) and its *Arabidopsis* homologs (Nakajima et al., 2006), although some methylated GAs, such as $MeGA_9$ and $MeGA_{73}$, appear to serve as bioactive molecules in ferns during the formation of antheridium (Yamauchi et al., 1996). The observation that transgenic *Arabidopsis* plants overexpressing *GAMT1* or *GAMT2* have lower levels of GAs, show varying levels of dwarfism, delayed flowering, and sterility and that these phenotypes can be partially reversed by the external application of GAs suggest that MeGAs are indeed inactive in *Arabidopsis* as well. We also directly tested the activity of $MeGA_4$ by applying it to the GAMT1-overexpressing lines and saw no amelioration in the dwarf phenotype.

Thus, methylation of GAs might be part of the mechanism affecting the levels of active GAs in developing siliques and/or seeds. It is possible that methylation of GAs is a step in the irreversible deactivation of GAs, perhaps tagging it for further catabolism by epoxidation, oxidation, or glycosylation, reactions known to occur in other parts of the plant or other plant species (Christmann and Doumas, 1998; Thomas et al., 1999; Zhu et al., 2006). Methylated GAs have a more hydrophobic character, and methylation thus may be necessary in part to allow the modified GAs to diffuse through membranes to reach their site of degradation. The lack of detection of MeGAs in both wild-type siliques and in leaves of plants overexpressing *GAMT1* also suggests that MeGAs are quickly converted to unknown metabolites, although a more extensive analysis of possible metabolites of the methylation reaction is required before a firm conclusion about the fate of MeGAs can be reached. The expression of *GAMT1* and *GAMT2* in the siliques peaks at the later stages of silique development, when the embryos in the siliques are nearing the end of their fast cell division and elongation, a process that is controlled by GAs, further suggesting a role for *GAMT1* and *GAMT2* in inactivation of GAs.

With some plant signaling molecules, methylation is known to be a reversible process. For example, an esterase that converts MeJA back to JA has been reported from tomato (*Solanum lycopersicum*) (Stuhlfelder et al., 2004) and potato (*Solanum tuberosum*) (accession number AY684102), and a related enzyme that hydrolyzes MeSA to SA has been reported from tobacco (Forouhar et al., 2005). Interestingly, the GA receptor recently reported from rice (Ueguchi-Tanaka et al., 2005) is a member of the same α/β-hydrolase superfamily to which the MeSA and MeJA esterases belong (Marshall et al., 2003), although it was reported that the angiosperm GA receptor is unlikely to be an active esterase. While it is possible that methylation of GAs, like GA glycosylation (Schneider et al., 1992), is in some cases a reversible process in plants, the results of the ancymidol inhibition experiments indicated that the wild-type *Arabidopsis* seeds were unable to recover the GAs that had been lost due to the activities of GAMT1 and GAMT2. Thus, the overall data we obtained in this study tentatively suggest that the function of methylating GAs in the developing seeds is in the irreversible inactivation of GAs. Since both *GAMT1* and *GAMT2* are expressed mainly in the developing siliques (including seeds), the enzymes they encode have partially overlapping substrate specificities, and double mutants show an additive effect of *GAMT1* and *GAMT2* expression on levels of some GAs, it can be concluded that the two genes have partially overlapping functions in silique and seed development. However, the specific physiological role of GA methylation in siliques, seeds, or in other parts of the plant remains to be determined.

METHODS

Plant Material and Growth Conditions

Wild-type *Arabidopsis thaliana* ecotype Col-0 was used in this study for all experiments. Plants were grown in soil or on MS basal salt medium containing 0.8 g/L agar with 12 h of light at 22°C and 12 h of dark at 18°C. cDNA clones and four SALK knockout mutant lines of *GAMT1* (SALK_088960 and SALK_047730) and *GAMT2* (SALK_109505 and SALK_143728) with Col-0 background were obtained from the ABRC (Alonso et al., 2003). Transgenic plants were obtained by *Agrobacterium tumefaciens*–mediated floral dip transformation (Clough and Bent, 1998) of wild-type plants (Col-0) with: cDNA of *GAMT1* or cDNA of *GAMT2* in sense orientation, driven by the cauliflower mosaic virus 35S promoter. Promoter-GUS transgenic plants with Col-0 background were used for histochemical analysis of GUS activity to monitor the expression pattern under *GAMT1*- and *GAMT2*-specific promoters.

For the ancymidol treatment experiment, dry *Arabidopsis* seeds stored for at least 1 month at room temperature were used. After sterilization, 50 to 100 seeds were placed on plates containing MS basal medium containing various concentrations of ancymidol (Sigma-Aldrich). Plates were placed at 4°C for 3 d and then transferred to a growth chamber at 22°C and a light/dark regime of 14/10 h, respectively, for 2 weeks.

For the qRT-PCR experiments, germinating seeds were obtained by placing seeds on soaked filter paper in the dark at 4°C for 3 d and then transferring the plate to 22°C in constant light for 48 h. At this point, the radicle began to protrude from the seeds and the material was harvested for RNA extraction.

Screening of T-DNA Insertion Mutants

The T-DNA insertion sites in the *GAMT1* and *GAMT2* genes were verified first by PCR (Siebert et al., 1995). For *GAMT1*, we used the genomic primers GAMT1 forward (5′-GGGAAGAAGCTAGCCGTGATTGACG-3′) and GAMT1 reverse (5′-CCACCGAAGAGATTGCGGCGGCGATTG-3′) to characterize the insertion lines SALK_047730 (designated here as *gamt1-1*) and SALK_088960 (designated as *gamt1-2*). For *GAMT2*, we used the primers GAMT2 forward (5′-GCCGGAGTTTGAGGCTTTCTTCTGTG-3′) and GAMT2 reverse (5′-GTTTTCCGCCATCCGAGTTTAA-3′) to characterize insertion lines SALK _143728 (designated here as *gamt2-1*) and SALK_109505 (designated as *gamt2-2*). In these experiments, we also used the T-DNA–specific primer LBB1 (5′-GCGTGGACCGCTTGCTGCAACT-3′). All PCR products were further verified by sequencing. Homozygous lines for the four mutants were confirmed by PCR with specific primers and subsequent DNA gel blot analysis.

Plasmid Construction

cDNA of *GAMT1* and *GAMT2* (ABRC) were cloned into the GATEWAY donor vector pDONR207 (Invitrogen). cDNA clones were transferred from pDONR207 to a destination vector pCHF3 (gift from Jianming Li, University of Michigan) modified with a GATEWAY cassette (Invitrogen). For expression of recombinant methyltransferases in *Escherichia coli*, cDNA clones *GAMT1* and *GAMT2* were transferred to pET28A vector (Novagen, EMD Biosciences), modified for GATEWAY.

RT-PCR and qRT-PCR Analyses

For RT-PCR analysis of the mutants, siliques half-way through maturation were used for extraction of total RNA (Maes and Messens, 1992). First-strand cDNA was synthesized by AMV reverse transcriptase (Promega) with poly(T)$_{18}$ primer. PCR was performed with 1 μL of the first-strand cDNA reaction. Specific forward and reverse primers for *GAMT1* were 5′-GGGAAGAAGCTAGCCGTGATTGACG-3′ and 5′-TACTACGCATGTTATGTACATATA-3′, respectively, and for *GAMT2* 5′-GCCGGAGTTTGAGGCTTTCTTCTGTG-3′ and 5′-TTAAACTCGGATGGCGGAAAAC-3′, respectively.

For qRT-PCR analysis, total RNA was isolated from different organs of *Arabidopsis* and from siliques at different stages of development as defined by Bowman (1994) using the RNA procedure described by Maes and Messens (1992). The RNA was subjected to DNase treatment using the DNA-free kit (Ambion), and first-strand cDNA was synthesized by AMV reverse transcriptase with poly(T)18 primer in parallel with a negative control reaction in which no AMV reverse transcriptase was added. All samples were brought to 100 μL in volume, after which 1 μL was used in a 20 μL of qPCR reaction containing 20 mM Tris, pH 8.4, 50 mM KCl, 3 mM $MgCl_2$, 5% DMSO, 250 μM deoxynucleotide triphosphate, 200 nM

primer, 0.5 units of Taq polymerase B (Promega), 1× CYBR-Green I dye (Molecular Probes),and 10 nM fluorescein (Bio-Rad). *GAMT1* and *GAMT2* gene-specific primers were designed as follows: *GAMT1* forward 5′-TGTTGTTTATGCTGATGGGTGGTC-3′ and *GAMT1* reverse 5′-CGCAATCTCTTCGGTGGTTCTAA-3′; *GAMT2* forward 5′-CGTCCTTCAGGCTCAAGTAGTC-3′ and *GAMT2* reverse 5′-CCCTATCTTGAAACCACCACAACGGTC-3′. Amplification of the ubiquitin gene ubq10 (At4g05320) using the forward primer 5′-AGGAGTCCACACTTCACTTGGTC-3′ and the reverse primer 5′-GGTGTCAGAGCTCTCTACCTCCA-3′ was used as internal control. The qPCR was performed on an iCycler thermocycler (Bio-Rad), with the following conditions: 95°C for 3 min, 50 cycles of 95°C for 15 s, 60°C for 30 s, and 72°C for 30 s, followed by a melting cycle of 55 to 95°C with an increasing gradient of 0.5°C, and a 10-s pause at each temperature. All reactions were performed in duplicate. Data processing was done by iCycler real-time detection system software (version 3.0). cDNA of RNA from siliques at half-way through development was serially diluted to generate the standard curve. Analyses of the melting curves were performed to ensure amplification of one specific gene product. At least three sets of independent experiments were performed to calculate a mean value and standard deviation. The cycle threshold (Ct) values generated by the iCycler software for each cDNA sample were used only when they met the following parameters: significant difference in Ct numbers between cDNA sample and the negative control was observed and the melting curve of the PCR product generated by the melting cycles was indicative of specific amplification.

Construction of Promoter-GUS Reporter Gene Fusion and Histochemical Localization of GUS Activity

The upstream regions of *GAMT1* and *GAMT2* were amplified from genomic DNA of *Arabidopsis*, cloned into pTOPO-ENTR, and subsequently transferred to pDW137 (Blazquez et al., 1997), modified for GATEWAY cloning by LR clonase reaction (Invitrogene). For *GAMT1*, the forward primer 5′-CACTTTGAAGAAGCGTGAGTGTAGGTAGTGC-3′ and the reverse primer 5′-GTTGTAAATGTGTAAGAAAAGGTGTGAACG-3′ were used to amplify a 1543-bp fragment upstream of the initiating ATG. For *GAMT2*, the forward primer 5′-GGATGGATAAATAGAGACATCGATCTG-3′ and the reverse primer 5′-GCTCTGTCTCTTCTCTCTTATTGGAAGTTGTAG-3′ were used to amplify a 1300-bp fragment. Five independent transgenic lines were obtained and tested for β-glucuronidase activity (Jefferson, 1987). Different plant organs were placed in staining solution containing 100 mM phosphate buffer, pH 7.0, 1 mM X-Gluc, 10 mM EDTA, 0.1% Triton-X and incubated at 37°C overnight. Plant material was destained with 70% ethanol. Cross-sectioning of GUS-stained siliques was performed with the JB-4 Plus embedding kit (Polysciences) using a protocol developed by Lee and Schiefelbein (2002).

Expression of *GAMT1* and *GAMT2* in *E. coli* and Protein Purification

Purification of GAMT1 and GAMT2 was performed by nickel–nitrilotriacetic acid agarose purchased from Qiagen. The expression and the purification procedure were performed by a modified procedure as described by Zubieta et al. (2003), but the elution step was the final step. The N-terminal His-tag was not cleaved for the subsequent methyltransferase assay. Purified protein of GAMT1 was used for production of rabbit polyclonal antibodies (Cocalico Biologicals).

Immunoblotting

Crude extracts were prepared from different stages of silique development or different parts from *Arabidopsis*. Immunodetection was performed using rabbit anti-GAMT1 polyclonal antibodies (1:2000 dilution). Goat anti-rabbit IgG horseradish peroxidase conjugate (1:20000 dilution) was used as a secondary antibody. Subsequent chemiluminescence was detected and exposed on Kodak BioMax XAR film using the Western Lightning Chemiluminiscence Reagent Plus kit (Perkin-Elmer Life Sciences).

Methyltransferase Enzyme Assay

The enzyme assay contained 1 μL of purified enzyme (~0.5 pmol), 10 μL of assay buffer (250 mM Bis-Tris-propane-HCl, pH 8.0, and 25 mM KCl), 1 μL of various GA substrates (prepared as a 50 mM solution in ethanol), 0.5 μL of ^{14}C-SAM (58 mCi/mmol; Perkin-Elmer), and water to a final volume of 50 μL. For a negative control, a boiled enzyme was used. The samples were incubated at 30°C for 30 min (over which period the reactions were linear), followed by extraction with 150 μL of ethyl acetate. The tubes were vortexed and briefly centrifuged, and 50 μL of the ethyl acetate phase were transferred to a scintillation vial containing 2 mL of scintillation fluid (Econo-Safe Research Products International) and counted in a scintillation counter (LS-6500 model; Beckman Coulter). For product verification, the same assay was scaled up to 500 μL using nonradioactive SAM for gas chromatography–mass spectrometry analysis or radioactive SAM for radioactive TLC. The nonradioactive products were twice extracted with 0.5 mL of ethyl acetate, dried under N_2 flow, and sylilated with 45 μL of pyridine and 60 μL of BSTFA (Sigma-Aldrich) for 30 min at 80°C and analyzed via the Shimadzu 5000 gas chromatograph–mass spectrometer. Separation was performed on an Altech EC-5 column (30 m × 0.32 mm × 1 μm). Helium was the carrier gas (flow rate of 2 mL min^{-1}), a splitless injection (3 μL) was used, and a temperature gradient of 4.5°C min^{-1} from 70°C (5-min hold) to 310°C was applied. The identities of methylated and sylilated GAs were determined by comparison of retention time and mass spectra to authentic sylilated standards.

Radioactive TLC was performed for all GAs described in the biochemical experiments as putative substrates for GAMT1 and GAMT2. A developing solution of chloroform and methanol in a ratio of 9:1 v/v was used as described by Roberts et al. (1999). The retention time of obtained radioactive products was compared with nonradioactive standards (prepared by L. Mander) or methylated GA standards with (trimethylsilyl)diazomethane (Sigma-Aldrich). For visualization of the nonradioactive GAs and their methylesters, the TLC plate was sprayed with sulfuric acid:ethanol (1:20 [v/v]) and then heated at 110°C for 10 min (Roberts et al., 1999).

Characterization of GAMT Kinetic Parameters

In all enzyme activity measurements, appropriate enzyme concentrations and incubation times were chosen so that the reaction velocity was linear during the incubation time period, and at least three replicates were performed. To determine the K_m value for each substrate (GA and SAM), one substrate concentration was fixed at a saturated level (1 mM), and the concentration of the other substrate to be measured was varied. Nine different concentrations were used. Lineweaver-Burk plots were performed to obtain the K_m and K_{cat} values.

To measure the pH optimum for GAMT activity, the reactions were performed in 50 mM Bis-Tris-propane-HCl buffer ranging from pH 6.0 to 9.5. Temperature stability of GAMT1 and GAMT2 was determined by incubating the enzymes at temperatures ranging from 4 to 65°C for 30 min and then chilling the samples on ice, followed by enzyme assays at 28°C.

Enzyme assays were performed with the following cations present in the assay buffer at the final concentration of 1 to 10 mM: Ca^{2+}, Cu^{2+}, Fe^{2+}, Fe^{3+}, K^{2+}, Mg^{2+}, Mn^{2+}, Na^{+}, NH_4^{+}, and Zn^{2+}.

GA and MeGA Measurements

Seeds from *Arabidopsis* Col-0 of the wild type, *gamt1*, *gamt2*, and *gamt1 gamt2* mutants, and overexpressing lines were sown in a Petri dish with MS medium supplemented with 10% sugar. After 2 weeks at 23°C, the seedlings were transplanted to soil and the plants were grown in a growth chamber at 23°C. For GA measurements for plants overexpressing GAMT1 and GAMT2, the aerial parts of plants that have just begun to

flower were collected. For GA measurements of siliques, siliques of developmental stages 5, 6, and 7 were collected.

Quantitative analysis of GAs for the first set of *GAMT1*-overexpressing lines and their wild-type control (Table 3) was performed by GC-SIM using ^{2}H-labeled GAs as internal standards as described previously (Gawronska et al., 1995). Briefly, an ethylacetate-soluble fraction containing GAs was subjected to HPLC purification using a reverse-phase column (Capcell Pak C18 SG120; Shiseido Fine Chemicals). When necessary, GA-containing fractions were then purified through another round of HPLC using an ion exchange column (Senshu Pak N[CH_3]$_2$, 1151-N; Senshu Scientific). The purified fractions were subjected to GC-SIM analysis using a mass spectrometer (Automass Sun; JEOL) equipped with a gas chromatograph (6890N; Agilent Technologies) and a capillary column (DB-1; Agilent Technologies) after derivatization.

GA measurements for other samples (Table 3, Figure 9) were conducted by liquid chromatography–selected reaction monitoring using ^{2}H-labeled GAs as internal standards. We used a liquid chromatography tandem mass spectrometry system consisting of a quadrupole/time-of-flight tandem mass spectrometer (Q-Tof Premier; Waters) and an Acquity Ultra Performance liquid chromatograph (Waters) equipped with a reverse-phase column (Acquity UPLC BEH-C18; Waters). Approximately 200 mg (dry weight) of lyophilized plant materials were used for each measurement. Details about the purification procedures and LC-MS/MS analysis conditions are described in Supplemental Methods and Supplemental Table 1 online.

Endogenous MeGAs were analyzed using ^{2}H-labeled MeGAs as internal standards by GC-SIM after derivatized to TMSi ester. Purification procedures of MeGAs from plant extracts are described in detail in the Supplemental Methods online.

Accession Numbers

The Arabidopsis Genome Initiative locus identifiers for genes mentioned in this article are as follows: *GAMT1* (At4g26420), *GAMT2* (At5g56300), and *IAMT1* (At5g55250). The updated annotation of At4g26420 will be available from TAIR and NCBI following the next genome release (TAIR7) scheduled for January, 2007.

Supplemental Data

The following materials are available in the online version of this article.

Supplemental Figure 1. Gas Chromatography–Mass Spectrometry of Authentic MeGA_{20} and the Product of the Methylation Reaction Catalyzed by GAMT1 and Using GA_{20} as the Substrate.

Supplemental Figure 2. Analysis of MeGAs in Wild-Type Siliques by GC-Selected Ion Monitoring Using [$^2H_2$]MeGAs as Internal Standards.

Supplemental Figure 3. Quantification of GAs by Selected Reaction Monitoring Using LC-MS/MS.

Supplemental Table 1. Parameters for GA Measurements by LC-MS/MS Analysis.

Supplemental Methods.

ACKNOWLEDGMENTS

We thank S.H. Kwak (University of Michigan) for help with the cross-sectioning of GUS-stained siliques and Jan Zeevaart (Michigan State University) for help with the early stages of the research. This work was supported by National Science Foundation Grants 0312466 to E.P., 0312449 to J.P.N., and 0312857 to V.S., by a Grant-in-Aid for Scientific Research (17770048) to S.Y. from the Ministry of Education, Culture, Sports, Science, and Technology of Japan, and by funds from the Pearlstein Fund for Research in Floriculture from the Hebrew University to R.B. and D.W.

Received June 6, 2006; revised November 22, 2006; accepted December 5, 2006; published January 12, 2007.

REFERENCES

Alonso, J.M., Stepanova, A.N., Leisse, T.J., Kim, C.J., Chen, H., Shinn, P., Stevenson, D.K., Zimmerman, J., Barajas, P., and Cheuk, R. (2003). Genome-wide insertional mutagenesis of *Arabidopsis thaliana*. Science **301:** 653–657.

Blazquez, M.A., Soowal, L.N., Lee, I., and Weigel, D. (1997). LEAFY expression and flower initiation in *Arasbidopsis*. Developopment **124:** 3835–3844.

Bowman, J. (1994). *Arabidopsis*: An Atlas of Morphology and Development. (Berlin: Springer-Verlag).

Chen, F., D'Auria, J.C., Tholl, D., Ross, J.R., Gershenzon, J., Noel, J.P., and Pichersky, E. (2003). An *Arabidopsis thaliana* gene for methylsalicylate biosynthesis, identified by a biochemical genomics approach, has a role in defense. Plant J. **36:** 577–588.

Christmann, A., and Doumas, P. (1998). Detection and identification of gibberellins in needles of silver fir (*Abies alba* Mill.) by combined gas chromatography-mass spectrometry. Plant Growth Regul. **24:** 91–99.

Clough, S.J., and Bent, A.F. (1998). Floral dip: A simplified method for *Agrobacterium*-mediated transformation of *Arabidopsis thaliana*. Plant J. **16:** 735–743.

Cowling, R., Kamiya, Y., Seto, H., and Harberd, N.P. (1998). Gibberellin dose–response regulation of *GA4* gene transcript levels in *Arabidopsis*. Plant Physiol. **117:** 1195–1203.

Curaba, J., Moritz, T., Blervaque, R., Parcy, F., Raz, V., Herzog, M., and Vachon, G. (2004). *AtGA3ox2*, a key gene responsible for bioactive gibberellin biosynthesis, is regulated during embryogenesis by *LEAFY COTYLEDON2* and *FUSCA3* in *Arabidopsis*. Plant Physiol. **136:** 3660–3669.

D'Auria, J.C., Chen, F., and Pichersky, E. (2003). The SABATH family of methyltransferases in *Arabidopsis thaliana* and other plant species. In Recent Advances in Phytochemistry, J. Romeo, ed (Oxford: Elsevier Science), 253–283.

Davies, P.G. (1995). Plant Hormones: Physiology, Biochemistry, and Molecular Biology. (Dordrecht, The Netherlands: Kluwer Academic Publishers).

Eeuwens, C.J., and Schwabe, W.W. (1975). Seed and pod wall development in *Pisum sativum* L. in relation to extracted and applied hormones. J. Exp. Bot. **26:** 1–14.

Eriksson, S., Bohlenius, H., Moritz, T., and Nilsson, O. (2006). GA_4 is the active gibberellin in the regulation of *LEAFY* transcription and Arabidopsis floral initiation. Plant Cell **18:** 2172–2181.

Fei, H., Zhang, R., Pharis, R.P., and Sawhney, V.K. (2004). Pleiotropic effects of the *male sterile33* (*ms33*) mutation in *Arabidopsis* are associated with modifications in endogenous gibberellins, indole-3-acetic acid and abscisic acid. Planta **219:** 649–660.

Forouhar, F., Yang, Y., Kumar, D., Chen, Y., Fridman, E., Park, S.W., Chiang, Y., Acton, T.B., Montelione, G.T., Pichersky, E., Klessig, D.F., and Tong, L. (2005). Structural and biochemical studies identify tobacco SABP2 as a methyl salicylate esterase and implicate it in plant innate immunity. Proc. Natl. Acad. Sci. USA **102:** 1773–1778.

Gawronska, H., Yang, Y.Y., Furukawa, K., Kendrick, R.E., Takahashi, N., and Kamiya, Y. (1995). Effects of low irradiance stress on gibberellin levels in pea seedlings. Plant Cell Physiol. **36:** 1361–1367.

Hedden, P., and Kamiya, Y. (1997). Gibberellin biosynthesis: Enzymes, genes and their regulation. Annu. Rev. Plant Phyiol. Plant Mol. Biol. **48:** 431–460.

Hedden, P., and Phillips, A.L. (2000). Gibberellin metabolism: New insights revealed by the genes. Trends Plant Sci. **5:** 523–530.

Huang, S., Raman, A.S., Ream, J.E., Fujiwara, H., Cerny, R.E., and Brown, S.M. (1998). Overexpression of 20-oxidase confers a gibberellin-overproduction phenotype in *Arabidopsis*. Plant Physiol. **118:** 773–781.

Jacobsen, S.E., and Olszewski, N.E. (1993). Mutations at the *SPINDLY* locus of Arabidopsis alter gibberellin signal transduction. Plant Cell **5:** 887–896.

Jefferson, R. (1987). Assaying chimeric genes in plants: The GUS gene fusion system. Plant Mol. Biol. Rep. **5:** 387–405.

Karssen, C.M., Zagórski, S., Kepczynski, J., and Groot, S.P.C. (1989). Key role for endogenous gibberellins in the control of seed germination. Ann. Bot. (Lond.) **63:** 71–80.

Kim, Y.C., Nakajima, M., Nakayama, A., and Yamaguchi, I. (2005). Contribution of gibberellins to the formation of Arabidopsis seed coat through starch degradation. Plant Cell Physiol. **8:** 1317–1325.

Lee, M.M., and Schiefelbein, J. (2002). Cell pattern in the *Arabidopsis* root epidermis determined by lateral inhibition with feedback. Plant Cell **14:** 611–618.

Lester, D.R., Ross, J.J., Smith, J.J., Elliott, R.C., and Reid, J.B. (1999). Gibberellin 2-oxidation and the *SLN* gene of *Pisum sativum*. Plant J. **19:** 65–73.

MacKenzie-Hose, A., Ross, J., Davies, N., and Swain, S. (1998). Expression of gibberellin mutations in fruits of *Pisum sativum* L. Planta **204:** 397–403.

Maes, M., and Messens, E. (1992). Phenol as grinding material in RNA preparations. Nucleic Acids Res. **20:** 4374.

Marshall, S.D., Putterill, J.J., Plummer, K.M., and Newcomb, R.D. (2003). The carboxylesterase gene family from *Arabidopsis thaliana*. J. Mol. Evol. **57:** 487–500.

Martin, D.N., Proebsting, W.M., and Hedden, P. (1999). The *SLENDER* gene of pea encodes a gibberellin 2-oxidase. Plant Physiol. **121:** 775–781.

Nakajima, M., et al. (2006). Identification and characterization of Arabidopsis gibberellin receptors. Plant J. **46:** 880–889.

Ogawa, M., Hanada, A., Yamauchi, Y., Kuwahara, A., Kamiya, Y., and Yamaguchi, S. (2003). Gibberellin biosynthesis and response during Arabidopsis seed germination. Plant Cell **15:** 1591–1604.

Olszewski, N., Sun, T.P., and Gubler, F. (2002). Gibberellin signaling: Biosynthesis, catabolism, and response pathways. Plant Cell **14**(Suppl)**:** S61–S80.

Qin, G., Gu, H., Zhao, Y., Ma, Z., Shi, G., Yang, Y., Pichersky, E., Chen, H., Lui, M., Chen, Z., and Qu, L.-J. (2005). Regulation of auxin homeostasis and plant development by an indole-3-acetic acid carboxyl methyltransferase in *Arabidopsis*. Plant Cell **17:** 2693–2704.

Rademacher, W. (2000). Growth retardants: Effects on gibberellin biosynthesis and other metabolic pathways. Annu. Rev. Plant Physiol. Plant Mol. Biol. **51:** 501–531.

Roberts, A.V., Blake, P.S., Lewis, R., Taylor, J.M., and Dunstan, D.I. (1999). The effect of gibberellins on flowering in roses. J. Plant Growth Regul. **18:** 113–119.

Ross, J.R., Nam, K.H., D'Auria, J.C., and Pichersky, E. (1999). S-adenosyl-L-methionine:salicylic acid carboxyl methyltransferase, an enzyme involved in floral scent production and plant defense, represents a new class of plant methyltransferases. Arch. Biochem. Biophys. **367:** 9–16.

Schmid, M., Davidson, T.S., Henz, S.R., Pape, U.J., Demar, M., Vingron, M., Scholkopf, B., Weigel, D., and Lohmann, J.U. (2005). A gene expression map of *Arabidopsis thaliana* development. Nat. Genet. **37:** 501–506.

Schneider, G., Jensen, E., Spray, C.R., and Phinney, B.O. (1992). Hydrolysis and reconjugation of gibberellin A_{20} glucosyl ester by seedlings of *Zea mays* L. Proc. Natl. Acad. Sci. USA **89:** 8045–8048.

Schomburg, F.M., Bizzell, C.M., Lee, D.L., Zeevaart, J.A.D., and Amasino, R.M. (2003). Overexpression of a novel class of gibberellin 2-oxidases decreases gibberellin levels and creates dwarf plants. Plant Cell **15:** 151–163.

Seo, H.S., Song, J.T., Cheong, J.J., Lee, Y.H., Lee, Y.W., Hwang, I., Lee, J.S., and Choi, Y.D. (2001). Jasmonic acid carboxyl methyltransferase: A key enzyme for jasmonate-regulated plant responses. Proc. Natl. Acad. Sci. USA **98:** 4788–4793.

Siebert, P.D., Chenchik, A., Kellogg, D.E., Kukyanova, K.A., and Lukyano, S.A. (1995). An improved PCR method for walking in uncloned genomic DNA. Nucleic Acids Res. **23:** 1087–1088.

Stuhlfelder, C., Mueller, M.J., and Warzecha, H. (2004). Cloning and expression of a tomato cDNA encoding a methyl jasmonate cleaving esterase. Eur. J. Biochem. **271:** 2976–2983.

Swain, S.M., Ross, J.J., Reid, J.B., and Kamiya, Y. (1995). Gibberellins and pea seed development. Planta **195:** 426–433.

Talon, M., Kornneeff, M., and Zeevaart, J.A.D. (1990). Endogenous gibberellins in *Arabidopsis thaliana* and possible steps blocked in the biosynthetic pathways of the semidwarf *ga4* and *ga5* mutants. Proc. Natl. Acad. Sci. USA **87:** 7983–7987.

Thomas, S.G., Phillips, A.L., and Hedden, P. (1999). Molecular cloning and functional expression of gibberellin 2-oxidases, multifunctional enzymes involved in gibberellin deactivation. Proc. Natl. Acad. Sci. USA **96:** 4698–4703.

Ueguchi-Tanaka, M., Ashikari, M., Nakajima, M., Itoh, H., Katoh, E., Kobayashi, M., Chow, T.Y., Hsing, Y.I., Kitano, H., Yamaguchi, I., and Matsuoka, M. (2005). *GIBBERELLIN INSENSITIVE DWARF1* encodes a soluble receptor for gibberellin. Nature **437:** 693–698.

Wang, H., Caruso, L.V., Downie, A.B., and Perry, S.E. (2004). The embryo MADS domain protein AGAMOUS-Like 15 directly regulates expression of a gene encoding an enzyme involved in gibberellin metabolism. Plant Cell **16:** 1206–1219.

Weigel, D., Ahn, J.H., Blazquez, M.A., Borevitz, J.O., Christensen, S.K., Fankhauser, C., Ferrandiz, C., Kardailsky, I., Malancharuvil, E.J., and Neff, M.M. (2000). Activation tagging in Arabidopsis. Plant Physiol. **122:** 1003–1013.

Weiss, D., Vanderluit, A., Knegt, E., Vermeer, E., Mol, J.N.M., and Kooter, J.M. (1995). Identification of endogenous gibberellins in petunia flowers – Induction of anthocyanin biosynthetic gene expression and the antagonistic effect of abscisic acid. Plant Physiol. **107:** 695–702.

Yamaguchi, S., and Kamiya, Y. (2000). Gibberellin biosynthesis: Its regulation by endogenous and environmental signals. Plant Cell Physiol. **41:** 251–257.

Yamauchi, T., Oyama, N., Yamane, H., Murofushi, N., Schraudolf, H., Pour, M., Furber, M., and Mander, L.N. (1996). Identification of Antheridiogens in *Lygodium circinnatum* and *Lygodium flexuosum*. Plant Physiol. **111:** 741–745.

Yang, Y., Yuan, J.S., Ross, J., Noel, J.P., Pichersky, E., and Chen, F. (2006). An *Arabidopsis thaliana* methyltransferase capable of methylating farnesoic acid. Arch. Biochem. Biophys. **448:** 123–132.

Yu, F., Park, S., and Rodermel, S.R. (2004). The *Arabidopsis* FtsH methaloprotease gene family: Interchangeability of subunits in chloroplast oligomeric complexes. Plant J. **37:** 864–876.

Zhu, Y., et al. (2006). *ELONGATED UPPERMOST INTERNODE* encodes a cytochrome P450 monooxygenase that epoxidizes gibberellins in a novel deactivation reaction in rice. Plant Cell **18:** 442–456.

Zimmermann, P., Hirsch-Hoffmann, M., Hennig, L., and Gruissem, W. (2004). GENEVESTIGATOR. *Arabidopsis* microarray database and analysis toolbox. Plant Physiol. **136:** 2621–2632.

Zubieta, C., Koscheski, P., Ross, J.R., Yang, Y., Pichersky, E., and Noel, J.P. (2003). Structural basis for substrate recognition in the salicylic acid carboxyl methyltransferase family. Plant Cell **15:** 1704–1716.